2 THEORY

2.1 Introduction

As with all analytical techniques a knowledge of the fundamental theory is necessary for a full interpretation of the results obtained. Building upon the introduction this chapter will explore in greater detail the expressions and equations which underpin field asymmetric ion mobility spectrometry (FAIMS). The chapter is separated into sections which deal with theory as a result of the ionisation, physical geometry, interactions between constituents and the electric field applied. Invariably there is overlap between these different categories and the links will be highlighted as they occur.

Throughout this chapter the default situation being described is of a FAIMS sensor with a single planar separation region. Many of the equations within this chapter are specific to a single orientation; for clarity the geometry of the default scenario is presented in Figure 2.1.

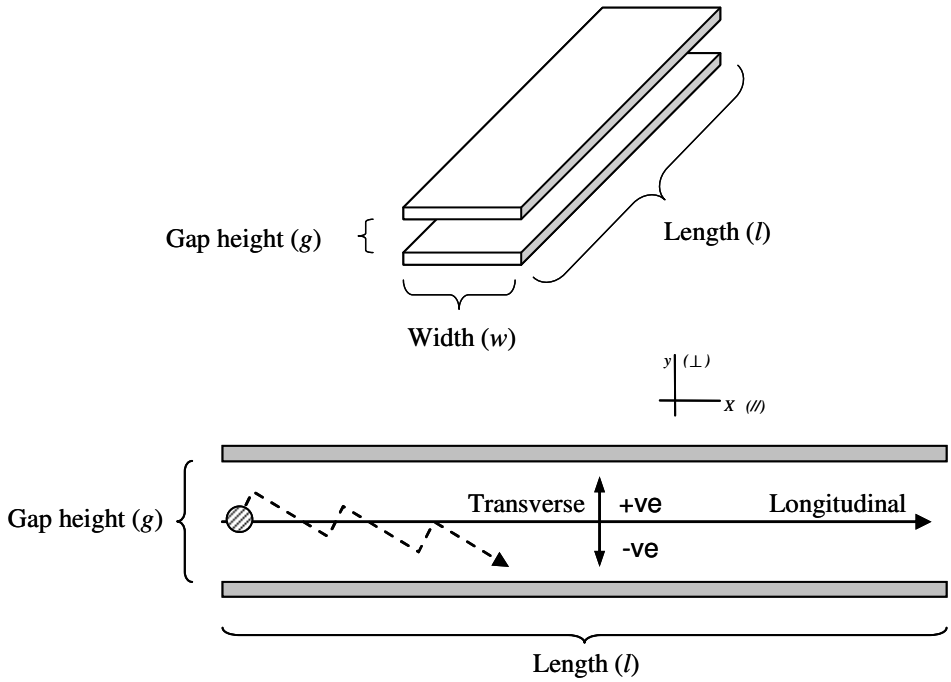

Figure 2.1 Defining the +ve and -ve direction with respect to the length and gap height of the separation region of a simple planar FAIMS device. An ion is depicted within the side-on view of the separation region and +ve reflects movement within the high field region, -ve is movement in the low field region.

2.2 Ionisation

Only species that are ionised can be separated and subsequently detected in a FAIMS system. The situation described below results from an ionisation source of ^{63}Ni and a carrier gas of air which is representative of the conditions of all the studies included within this thesis.

Since FAIMS devices operate under non-vacuum environments the ionisation mechanism is a result of interactions not only with the sample under study but also the carrier gas employed. The processes for the formation of the positive and negative reservoir/reactant ions and positive and negative product ions are presented.

Much of this section is derived from two sources, in particular the formation of reactive ions from Good *et al*. [1] and formation of product ions from Eiceman and Karpas [2].

2.2.1 Formation of positive reactive ions

Direct excitation, via the impact of electrons, results in the ionisation of the neutral components of the carrier gas. Positive reactive ions are generated by ionisation of nitrogen (N_2).

$$N_2 + e^-(primary) \rightarrow N_2^+ + e^-(primary) + e^-(secondary) \qquad 2.1$$

The average energy of the primary and secondary electron is 17 and 1 keV which means that a single primary electron can eventually be responsible for 500 N_2 ionisations (since 35 eV is required to produce an ion pair) [2]. The ionised N_2 goes on to excite water molecules present through the reactions described by Equations 2.2 - 2.4.

$$N_2^+ + 2N_2 \rightarrow N_4^+ + N_2 \qquad 2.2$$

$$N_4^+ + H_2O \rightarrow 2N_2 + H_2O^+ \qquad 2.3$$

$$H_2O^+ + H_2O \rightarrow H_3O^+ + OH \qquad 2.4$$

The hydrated proton is the reactive ion which forms a reservoir with which analyte ions can interact with and form the final product ions (Section 2.2.3).

Low levels of water vapour in the source result in long lifetimes of N_2^+, H_2O^+ or N_4^+. This in turn may result in a charge transfer reaction with other molecules in the reaction region [3]. Equation 2.5 uses N_2^+ as an example for such a charge transfer reaction.

$$N_2^+ + Z \rightarrow N_2 + Z^+ \qquad 2.5$$

Where *Z* can be any other neutral molecule present *e.g.* O_2 or analyte.

2.2.2 Formation of negative reactive ions

Negative reactant ion formation involves both the main constituents, nitrogen and oxygen. Low energy electrons that are thermalised with the neutral carrier gas of air can attach to oxygen through three-body collisions. Here *Z* is a neutral molecule (where N_2 is the most abundant) which is required to share momentum with the constituents but otherwise does not take part in the reactions described by Equations 2.6 - 2.8.

$$O_2 + e^- + Z \rightarrow O_2^- + Z \qquad 2.6$$

$$H_2O + O_2^- + Z \rightleftharpoons O_2^- H_2O + Z \qquad 2.7$$

$$H_2O + O_2^- H_2O + Z \rightleftharpoons O_2^- (H_2O)_2 + Z \qquad 2.8$$

The $O_2^-(H_2O)_n$ ion generated is the negative reactant ion which then interacts with the analyte.

2.2.3 Formation of positive product ions

The hydrated proton, $H^+(H_2O)$, created within Equation 2.4 can be further hydrated through additional reactions with water. It is therefore more appropriate to denote the reactive ion with a general expression, $H^+(H_2O)_n$, where *n* is a natural number.

Collisions of the hydrated proton species and analyte molecules, *M*, can result in an intermediary adduct ion. This transition state may dissociate back to its reactants or may go on to form product ions. A third body is again required to stabilise the products. This process is described by Equation 2.9.

$$H^+(H_2O)_n + M + Z \rightleftharpoons \underset{\text{TRANSITION STATE}}{\left[MH^+(H_2O)_n\right]^*} + Z \rightleftharpoons MH^+(H_2O)_{n-1} + H_2O + Z \qquad 2.9$$

The rate at which product ions are formed is dependent upon the collision frequency and the concentration of reactant ions, analyte molecules and the presence of suitable species to act as *Z*.

As the concentration of analyte is increased the reservoir of reactant ions decreases, and the population of positive product ions increases. If the concentration of analyte ions is increased it may be possible for another analyte molecule to unite with the original product ion as in Equation 2.10.

$$MH^+(H_2O)_n + M \rightleftharpoons M_2H^+(H_2O)_{n-1} + H_2O \qquad 2.10$$

Clustering with $(N_2)_m$ has also been described [4].

It is convention to refer to product ions with a single analyte molecule as a *monomer* and a product ion with two analyte molecules as a *dimer*.

2.2.4 Formation of negative product ions

Mirroring the process that occurred with positive polarity the negative reactant ions can undergo further hydration so that a general expression of $O_2^-(H_2O)_n$ is more appropriate. Just as in Equation 2.9 this reactant ion can go on to form a transition state which may then form the negative product ion.

$$O_2^-(H_2O)_n + M + Z \rightleftharpoons \underset{\text{TRANSITION STATE}}{\left[MO_2^-(H_2O)_n\right]^*} + Z \rightleftharpoons MO_2^-(H_2O)_{n-1} + H_2O + Z \qquad 2.11$$

Eiceman and Karpas have reported that other processes can occur [2]. These include:

$$O_2^-(H_2O)_n + M + Z \rightleftharpoons \left[MO_2^-(H_2O)_n\right]^* + Z \rightleftharpoons M^-(H_2O)_n + O_2 + Z \qquad 2.12$$

$$O_2^-(H_2O)_n + M + Z \rightleftharpoons \left[MO_2^-(H_2O)_n\right]^* + Z \rightleftharpoons (M-1)^-(H_2O)_n + HO_2 + Z \qquad 2.13$$

Where Equation 2.12 is a charge transfer reaction and Equation 2.13 is a proton abstraction that requires the analyte to contain hydrogen.

2.3 Types of interaction

Nazarov *et al*. presented five separate ways in which the field dependence of the mobility coefficient could be understood [5]. Considering the consequence of separate effects upon the mobility coefficient is important as it is the principal quantity that results in the separation of compounds within a FAIMS sensor. These mechanisms consider the carrier flow and applied asymmetric waveform. This section is intended as an introduction with a more in depth treatment provided later in the chapter for the most prevalent types of interaction.

2.3.1 Scattering through direct contact

Considering the ions and neutral carrier flow as rigid bodies has been the standard approach to understanding mobility. This methodology is explored in greater detail within Section 2.4.2.

2.3.2 Elastic scattering due to polarisation interaction

As ions move through the carrier gas they can induce a dipole in the neutral species present. Interaction between ions and induced dipoles can then occur and is dependent upon an effective ion neutral cross section (Ω_{pol}). This cross section is dependent upon the relative velocities of the constituents, with the interaction becoming more likely if the constituents are moving slowly [6],

$$\Omega_{pol} \propto \frac{1}{\sqrt{\varepsilon}}. \qquad 2.14$$

Where ε is the energy of the ion.

When the effective ion neutral cross section decreases to the geometric size of the constituents the effect through induced dipoles should no longer be in evidence and scattering through direct contact is dominant.

2.3.3 Resonant charge transfer

When ions are similar in structure to the neutral species present in the carrier flow the transfer of electrons can easily occur between the constituents. This happens very quickly and when it occurs an ion's velocity is lost. Charge transfer will therefore affect the drift velocity of an ion. Nazarov *et al*. noted that the theory resulting from scattering through direct contact also describes the effects of resonant charge transfer [5].

2.3.4 Change in shape/identity of ion

High electric fields potentially have the energy to change the molecular conformation and dipole moments of species. Such changes to the shape of an ion are often abrupt as the energy imparted to the ion reaches a critical value. An example of this is the response from methyl salicylate given in Figure 2.2.

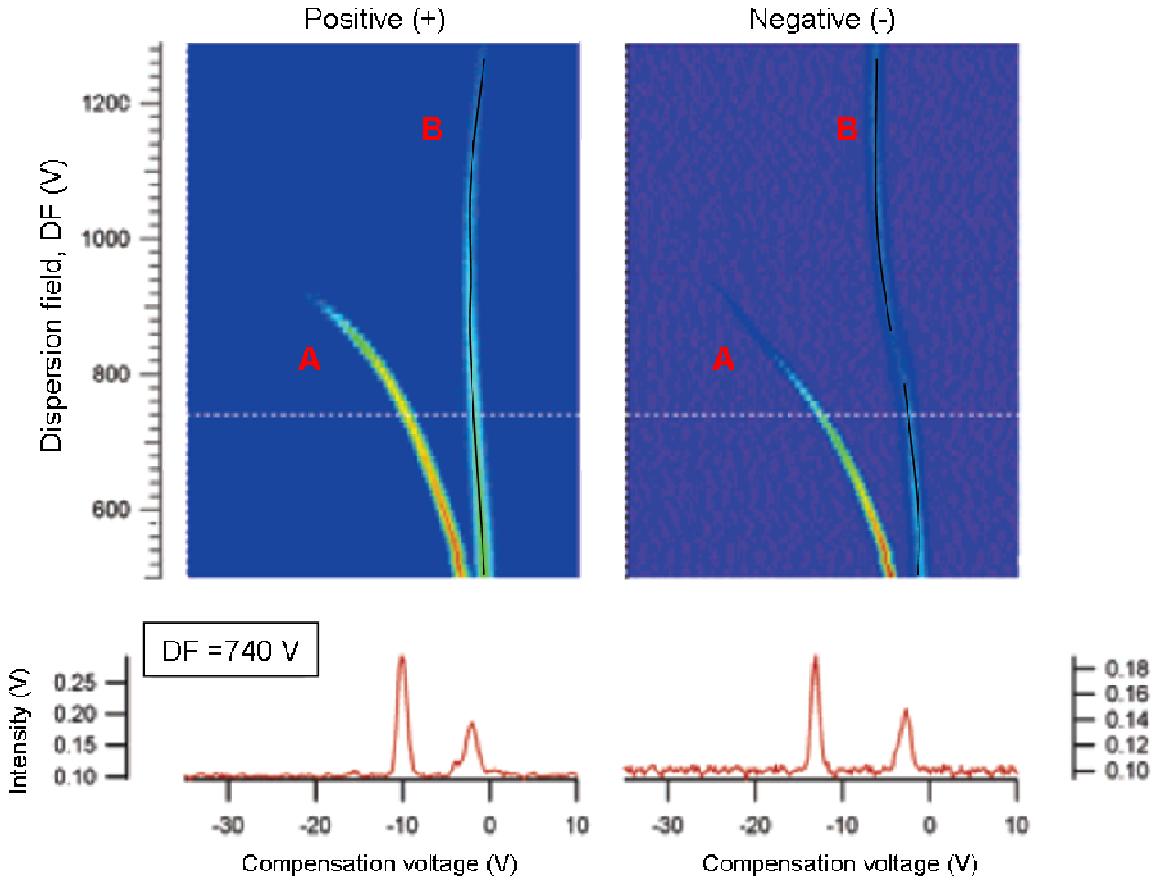

Figure 2.2 DF sweeps of methyl salicylate in positive and negative polarity. **A** are the reactant ions and **B** are the product ions. The dispersion field has units of volts because the gap height is fixed, meaning that the only variable is voltage. Originally from Nazarov *et al* [5]. Black lines have been added to the track from the product ions to help distinguish signal from background.

The response from all the reactant and product ions appears to be smooth and continuous except for the product ion peak in the negative polarity. The apparent break in the negative product ion peak was suggested as a consequence of the applied electric field changing the identity of the product ion. Through the use of a mass spectrometer this hypothesis was

confirmed. The expected product ion was indeed changed through a proton abstraction as a consequence of heating of the ion [5, 7].

2.3.5 Clustering and de-clustering of ions

While ions traverse the separation region of a FAIMS sensor an asymmetric waveform is cycled. This results in the ions experiencing differing environments at different times. For instance, the low field portion of the waveform may be more conducive to the solvation of neutrals onto the molecular ion cluster. In contrast the high field portion may make the likelihood of such clustering unlikely. If this scenario were to occur an increase in the collision cross section would be expected in a low field but not in a high field. Such a change would affect the difference in mobility experienced by the ion throughout the waveform and result in a change of observed ion behaviour. The effect would be dependent upon the chemical identity of the ions and available neutrals. Solvation is likely if the Gibbs energy of the solvated system is less than the case with no solvation [8].

The onset of clustering has been investigated by increasing the population of potential clustering neutrals. It was discovered that the onset of clustering occurred at a set-point which was dependent upon the concentration of potential clustering neutrals and the frequency of the asymmetric waveform [9]. The hypothesis of this ‘solvent effect’ has since been questioned by Shvartsburg [10] and the two arguments are discussed in Appendix A. Through work presented later within Chapter 5 the solvent effect appears to explain likely clustering behaviour. It is suggested that the conflict within the literature can be settled with the inclusion of a term describing the rate that which collisions are successful. This is present within the work by Eiceman and Kapras but not Schvartsburg.

There have also been a number of studies investigating the possibility of exploiting clustering to better resolve separate ion species [9, 11-13].

2.4 Drift velocity

Fundamental to the separation of ions of different species is the assertion that in an electric field ions of separate species drift at unique velocities [14]. This was first introduced in Chapter 1 (Section 1.4) but the key expressions are repeated here to aid with the discussion.

The velocity of each ion species is a drift velocity (v_d) and is the product of the electric field strength (E) and the mobility coefficient (K) which is exclusive for every ion species.

$$v_d = KE \qquad 1.1$$

Within this section different approaches to describing the mobility coefficient and drift velocity are presented. This allows for an understanding of the dependence on separate variables not present within a single description.

2.4.1 Symmetry considerations

The mobility coefficient is typically reported as dependent upon the summation of high and low electric field terms [6].

$$K(E/N) = K_0(0)[1 + \alpha(E/N)] \quad 1.6$$

$$K(E/N) = K_0(0)\sum_{n=1}^{\infty} \alpha_n \left[\left(1 + (E/N)^{2n}\right)\right] \quad 2.15$$

$$K(E/N) = K_0(0)\left[1 + \alpha_1(E/N)^2 + \alpha_2(E/N)^4 + ...\right] \quad 1.7$$

Where N is the number density of neutrals.

The α values within Equations 2.15 and 1.7 are all coefficients of expansion and K_0 is the mobility coefficient at low field strength. The α function within Equation 1.6 is different and can be used to describe the change in the mobility coefficient across a range of *E*/*N*.

Of interest is the realisation that upon expansion of the mobility coefficient (through a power series) only even powers are included. The reason for this is that the symmetry of Equation 1.1 results in the mobility coefficient always being positive, so only even powers are possible. This is explained with the aid of Figure 2.1 where the direction of the high field electric field acting in the positive direction is defined. If this co-ordinate system was reversed, so that the high strength electric field was now said to be acting in the negative direction by the same transformation, the velocity of an ion swarm which was previously positive would now be negative. By Equation 1.1, the resultant mobility coefficient remains positive despite the redefinition of the co-ordinate system. Odd powers of the expansion could result in a negative mobility coefficient and so are impossible.

2.4.2 Momentum transfer theory

Collisions between ions and neutral molecules are considered the primary physical mechanism for interaction of ions within the separation region. To investigate this interaction the theory of momentum transfer is applied [6].

A full treatment is provided within Appendix B but the final result is that the average velocity of ions can be described by the sum of three components, as described by Equation 2.16.

$$\frac{1}{2}m\bar{v}^{2} = \frac{1}{2}M\bar{V}^{2} + \frac{1}{2}mv_d^2 + \frac{1}{2}Mv_d^2 \qquad 2.16$$

Where v_d is the drift velocity of the ions, m and $\bar{v}$ are the mass and average velocity of the ions respectively and M and $\bar{V}$ are the mass and average velocity of the neutral molecules respectively.

The terms on the right hand side of Equation 2.16 represent real world observable quantities. The first term is only dependent upon the mass and velocity of the neutral gas and so is determined by the thermal environment and is equal to $\frac{3}{2}k_bT$. The second term is the drift motion of ions while the third term is the random part of the field energy due to the effects of any collision that occurs.

2.4.3 Drift velocity through constant acceleration

FAIMS theory is usually used to describe the velocity of an ion swarm instead of individual ions because it is more representative of the outputs from a FAIMS sensor. This is attributable to the large number of interactions with the neutral supporting atmosphere

which results in a velocity profile. This means that it is best to describe the velocity of the population as opposed to individual ions.

There are different ways of expressing the drift velocity which enable various insights into the separation of ions within a FAIMS instrument. One approach assumes a constant acceleration of ions between collisions with the neutral carrier flow, the drift velocity is then described by,

$$v_d = \left(1 + \frac{m}{M}\right)\frac{eE}{m}\tau = \frac{eE}{\mu}\tau \qquad 2.17$$

Where τ is the mean free time between collisions, m is the mass of the ion, M is the mass of the neutral and μ is the reduced mass. A full derivation of Equation 2.17 is provided in Appendix C.

Through this description it is now possible to obtain some simple expressions for scenarios with respect to the identity of carrier gas and ions of interest.

When: $M \geq m$,

$$v_d \approx \frac{eE}{m}\tau \qquad \text{(light ions)} \qquad 2.18$$

When $m \geq M$,

$$v_d \approx \frac{eE}{M}\tau \qquad \text{(heavy ions)} \qquad 2.19$$

The mean free path is dependent upon the number density and therefore the pressure within the separation region. By equating Equation 1.1 to 2.17 it becomes clear that increasing the time between collisions (*i.e.* decreasing the pressure) results in an increase in the mobility coefficient resulting in larger separation of ion species. Changing the carrier gas used can also have a beneficial effect and is most relevant when $m \geq M$ as described by Equation 2.19.

2.4.4 Drift velocity through mean free path

Equation 2.17 is useful but it is possible to take the understanding of drift velocity and therefore the mobility coefficient further. Owing to the complicated interactions that can occur within a FAIMS device between ions and the neutral carrier gas, Equation 2.17 is often modified to incorporate a factor, ζ, and placed in terms of the collision cross section (Ω). ζ is a factor that is included to represent any constants resulting from the ion-molecule interaction and is useful to be kept as indeterminate for manipulation. The following derivation is used extensively throughout the understanding of IMS and FAIMS and this reproduction is based upon the work by Mason and McDaniel [6, 15].

The mean free time of the ions within the separation region can be expressed by,

$$\frac{1}{\tau} = \bar{v}_r N \Omega \qquad 2.20$$

where τ is the mean free time and $\bar{v}_r$ is the average relative velocity of the ions with the neutral molecules.

As a reminder, the quantity $\bar{v}_r$ is not the drift velocity introduced within Equation 1.1 and instead it is a result of the mean velocities of the ions and neutral gas molecules. The relative velocity is approximately related to the ion velocity (v) and gas molecule velocity (V) through the equation,

$$\bar{v}_r^2 = \overline{(v - V)^2} = \bar{v}^2 + \bar{V}^2 \qquad 2.21$$

Substituting Equations 2.20 and 2.21 into Equation 2.17 and also introducing the factor ζ gives the expression,

$$v_d = \zeta\left(\frac{1}{m}+\frac{1}{M}\right)\frac{eE}{\left(\overline{v}^2+\overline{V}^2\right)^{1/2}N\Omega} \qquad 2.22$$

Under low field conditions (*e.g.* an IMS system or low field strength region of a FAIMS device) the energy of the ions and molecules between collisions is comparable to the thermal energy of the gas,

$$\frac{1}{2}mv_d^2+\frac{1}{2}Mv_d^2 \approx \frac{3}{2}k_bT \qquad 2.23$$

Combining Equations 2.22 and 2.23 and then substituting into Equation 2.22 provides an expression that better describes the parameters controlling the drift velocity as observed within a FAIMS device.

$$v_d = \frac{\zeta}{3^{1/2}}\left(\frac{1}{m}+\frac{1}{M}\right)^{1/2}\frac{e}{(k_bT)^{1/2}\Omega}\left(\frac{E}{N}\right) \qquad 2.24$$

For high field strength regimes the largest energy contribution to ions and molecules is the energy resulting from the electric field on the ions. While $\overline{v^2}$ has a negligible thermal component some of the energy is still randomised through interaction with the neutral carrier gas. In a high field system where the mass of ions is approximately the same as the mass of the neutral molecules, $m = M$. Thus,

$$\frac{1}{2}mv_d^2+\frac{1}{2}Mv_d^2 \approx \frac{1}{2}M\overline{v^2} \qquad 2.25$$

Combining Equations 2.22 and 2.25 and substituting into Equation 2.22 the drift velocity for high field regions is obtained.

$$v_d = \zeta^{1/2}\left(\frac{1}{m}+\frac{1}{M}\right)^{1/4}\left(\frac{e}{M^{1/2}\Omega}\right)^{1/2}\left(\frac{E}{N}\right)^{1/2} \qquad 2.26$$

Equations 2.24 and 2.26 are expressions for the drift velocity in separate parts of a FAIMS waveform while Equation 2.17 has no such distinction. Including the effects of a high and low field region a changing dependence on the ratio of *E*/*N* is found. Through Equations 2.24 and 2.26 it is also easier to appreciate the effect of a changing collision cross section and the difference with respect to electric field strength and molecular number density dependence in a low and high field:

$$v_d \propto \frac{E}{N} \qquad \text{(low field)} \tag{2.27}$$

$$v_d \propto \left(\frac{E}{N}\right)^{1/2} \quad \text{(high field)} \tag{2.28}$$

In addition, the collision cross section can depend on the electric field strength (Section 2.3.5) and the factor ζ can have a mass dependence. Studies have discovered that the factor ζ in low fields is equivalent to [16],

$$\zeta = \frac{3}{16}(6\pi)^{1/2} = 0.814 \tag{2.29}$$

and within high fields as [17],

$$\zeta = \frac{(1.1467)^2}{2^{1/2}} = 0.930 \tag{2.30}$$

Combining the drift velocity equations for low field conditions (*i.e*. Equations 2.24 and 2.29) then placing in terms of mobility (Equation 1.7) a widely used expression, commonly referred to as the Mason-Schamp equation [18-20], is resultant.

$$K = \frac{3e}{16}\left(\frac{2\pi}{k_b T}\right)^{1/2}\left(\frac{1}{m}+\frac{1}{M}\right)^{1/2}\frac{1+\alpha}{\Omega}\left(\frac{E}{N}\right) \tag{2.31}$$

2.5 Energy

The earlier treatments of drift velocity described the motion of ions being dependent upon the drift velocity. Within the separate low and high field regions, ion motion was described as principally being a result of the energy from the thermal environment and the electric field. Just as different approaches to the drift velocity yielded different perspectives, considering the energy experienced by ions provides new insight.

2.5.1 Weak or strong field

FAIMS systems separate ions through the application of an asymmetric waveform being applied as ions travel through the separation region. The separation requires that the ions undergo regions of low and high electric field strengths so that a change in mobility manifests. Energy can go into ion or thermal motion. A weak field results if the energy imparted to the ions within the separation region $(\Delta\varepsilon_i)$ is less than the energy of the thermally excited neutrals present, *i.e.* $\Delta\varepsilon_i < k_b T$. In this situation energy imparted to ions that could result in ion motion is masked by the induced random movement through interaction with the more energetic neutrals.

If the energy imparted to the ions through the electric field is much greater than that available to the neutrals, *i.e.* $\Delta\varepsilon_i >> k_b T$, the electric field is said to be of strong strength. This means that the energy imparted to the ions, due to the electric field, is unlikely to be masked by random motion and a drift velocity of the ions will be dependent upon the imposed field.

2.5.2 Interactions between ions and neutrals

This treatment is similar to the previous focus on the impact on the ion drift velocity by collisions with the neutral carrier flow (Section 2.4.3). To prevent repetition, the bulk of this discussion is included in Appendix D. An important result is that the energy imparted to the ions is dependent upon the ratio *E*/*N*.

$$\Delta\varepsilon_i = eE\lambda = \frac{e}{\Omega}\left(\frac{E}{N}\right) = k_b T \frac{eE}{\Omega P} \qquad 2.32$$

Where $\Delta\varepsilon$ is the change in energy, k_b is the Boltzmann constant, T is the temperature and P is the pressure.

E/*N* occurs throughout FAIMS theory and while the ratio is made up of two independently controlled variables, the ratio can be treated as a single variable. Theoretically the ratio defines the energy imparted to the ions and therefore describes a fundamental measure of the ions behaviour. Only through clustering and dipole alignment can the mobility of ions change without being dependent upon the ratio *E*/*N* [10].

The variables of electric field strength and number density of neutrals can rarely be separated because they both directly affect the energy experienced by an ion. The electric field accelerates the ion between collisions with the neutral carrier gas and the number density describes how often the collisions occur which removes the gained energy (and hence its velocity).

2.5.3 *E*/*N* ratio

Nazarov *et al*. demonstrated the importance of the ratio of *E*/*N* on the interpretation of the results obtained in a FAIMS system through explaining the effects of modifying the

pressure, and hence the number density of the carrier flow [5]. Figure 2.3 is a plot taken from that study plotting the position of ion response while varying the pressure of carrier flow used.

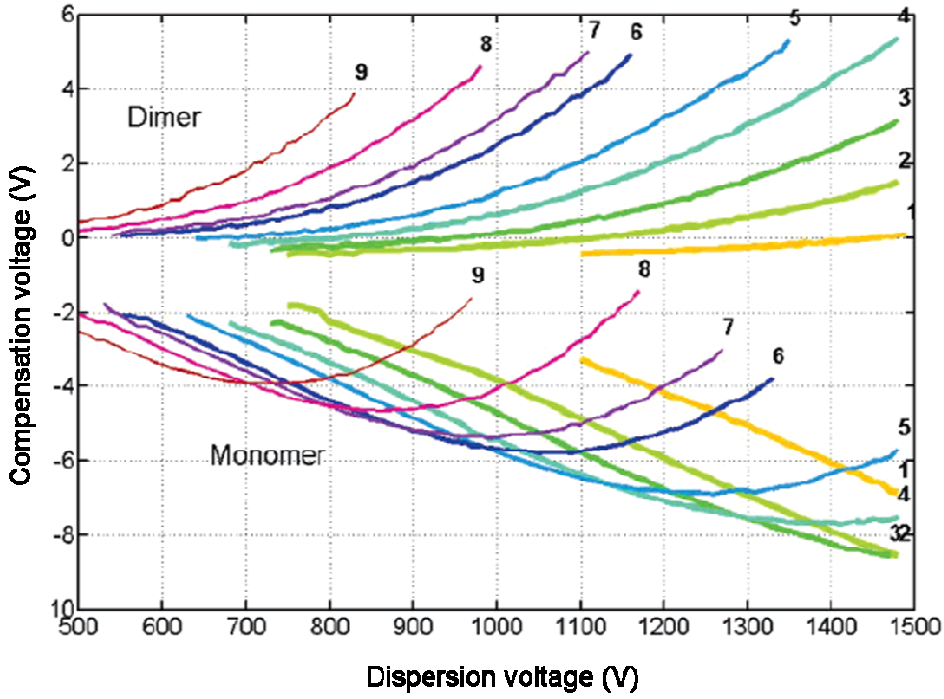

Figure 2.3 Dimethylmethylphosphonate monomer and dimer peak positions at a range of pressures (curves labelled 1 -9 were obtained with pressure values of 1.555, 1.185, 1.006, 0.859, 0.764, 0.638, 0.592, 0.512 and 0.422 atm, respectively). Dispersion voltage is the voltage required for the imposed dispersion field. Originally from Nazarov *et al* [5].

It appears that all the ion responses are independent of one another. When the CV position is measured in terms of Townsends (Td), which is the unit of the *E*/*N* ratio (1 Td = 1×10^{-17} V·cm^2), the results given in Figure 2.4 are obtained. Describing the data by the Townsend unit normalises the data to the ratio *E*/*N*.

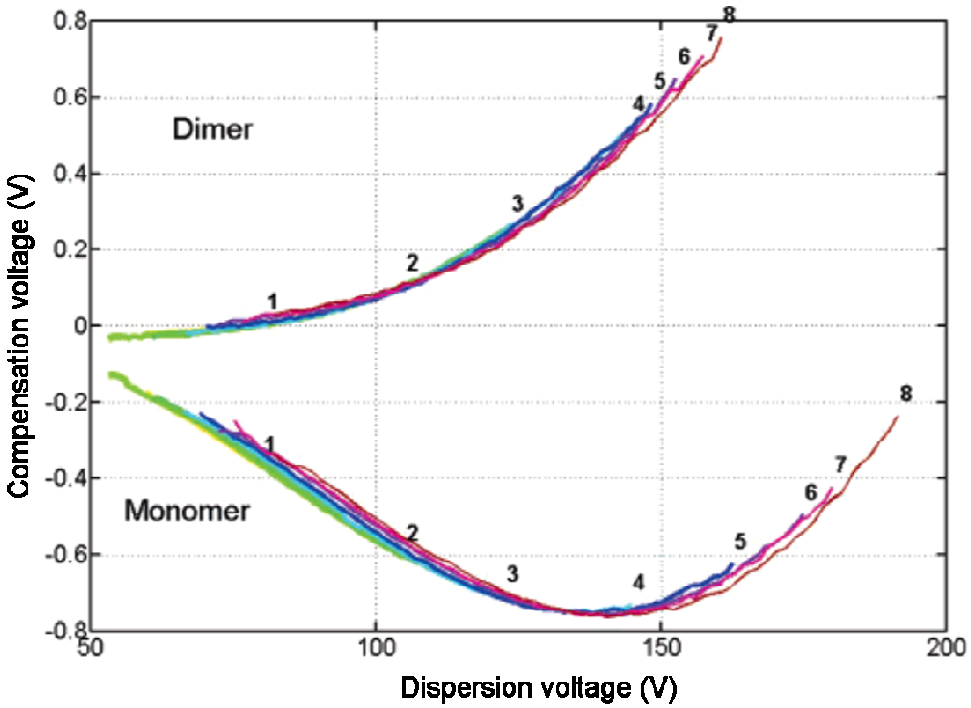

Figure 2.4 Townsend scaled dimethylmethylphosphonate monomer and peak positions for a range of pressures (curves labelled 1 -8 were obtained with pressure values of 1.555, 1.185, 1.006, 0.859, 0.764, 0.638, 0.592 and 0.512 atm, respectively). Dispersion voltage is the voltage required for the imposed dispersion field. Originally from Nazarov *et al* [5].

Despite the various electric fields and pressures of carrier flow it is shown that the position of the ions response, which is a result of the drift velocity of the ions, is dependent upon the *E*/*N* ratio only. Since the *E*/*N* ratio can be treated as a single variable it does not matter how the ratio is changed, thus halving the number density has the same effect as doubling the electric field strength.

Nazarov *et al*. suggest *E*/*N* scaling as standard presentation of FAIMS spectra as it enables direct comparison of spectra obtained under different experimental conditions and even various sensor designs [5]. Furthermore, Nazarov *et al*. describe the effect upon the translational and longitudinal velocity of ions, this work is re-counted in Appendix E.

2.6 Physical properties

While the motion of ions within the separation region of a FAIMS instrument is critically dependent upon the electric fields applied, the physical dimensions of the separation region are also important.

2.6.1 Residence time

Residence time (t_{res}) is the time spent by an ion within the separation region of a FAIMS device. The translational velocity of the ion through the separation region is only dependent upon the magnitude of the carrier flow and the dimensions of the separation region. All imposed electric fields are orthogonal to the translational component of the ion so residence time is independent of field and may be calculated through,

$$t_{res} = \frac{gwl}{Q} = \frac{V_m}{Q} \qquad 2.33$$

Where V_m is the volume of the separation region, Q is the volume flow rate and g,w and l are dimensions as defined in Figure 2.1.

The greater the residence time the longer the ions will be subject to the filtering influence of the electric fields. Therefore as the residence time increases the resolution and selectivity of the FAIMS system increases. At the same time, increased residence allows for more random interactions (collisions) of ions with the neutral carrier gas, which leads to greater losses to an electrode. Consequently, there is typically an associated loss of sensitivity with increased selectivity. Diffusional losses are covered in more detail within Section 2.9.

2.6.2 Reynolds number and turbulent flow

The flow path through an experiment is rarely geometrically constant. There will be points of restriction and points where the flow is less constrained. It is desired that the flow through the separation region is laminar as turbulent flow of the neutral gas would affect the orthogonal motion of the ions and therefore the ion response obtained from the instrument. To approximate how turbulent a flow is the Reynolds equation is usually employed.

Schlichting showed that the velocity at some point in the velocity field (u) is proportional to the mean free stream velocity ($\overline{V}$). The velocity gradient ($\partial u / \partial x$), is proportional to ($\overline{V} / g$), and similarly ($\partial^2 u / \partial y^2$) is proportional to ($\overline{V} / g^2$). Hence the ratio,

$$\frac{Inertia}{Friction} = \frac{\rho u \partial u / \partial x}{\mu_d \partial^2 u / \partial y^2} = \frac{\rho \overline{V}^2 / g}{\mu_d \overline{V} / g^2} = \frac{\rho \overline{V} g}{\mu_d} \qquad 2.34$$

Where μ_d is the dynamic viscosity and ρ is the density.

Therefore, the condition of similarity is satisfied if the quantity $\rho \overline{V} g / \mu_d$ is equivalent between two separate flows. Such a result would describe two systems with an equal degree of turbulence.

This principle was discovered by Osborne Reynolds when he investigated fluid motion through pipes and is, therefore, known as the Reynolds principle of similarity. The dimensionless ratio is called the Reynolds number (Re). Here the ratio of the dynamic viscosity to the density, described by $v_k = \mu_d / \rho$, is the kinematic viscosity of the fluid.

It is generally considered that a $Re > 3000$ represents a turbulent flow and anything below is a laminar flow [21]. The Reynolds number as expressed by the kinematic viscosity is,

$$\mathrm{Re} = \frac{\rho \bar{V} g}{\mu_d} = \frac{\bar{V} g}{v_k} \qquad 2.35$$

The v_k of air and N_2 at STP is ~ 17×10^{-5} $m^2 s^{-1}$ [10].

FAIMS devices do not usually suffer from turbulent flow within the separation region since their development was driven by miniaturisation and so the quantity of gap height (g) is usually sufficiently small enough to ensure laminar flow. For example, the Owlstone FAIMS sensor ($g = 35 \times 10^{-6}$ m) with a carrier flow of air under standard conditions at a flow rate of 5 l/min has a Reynolds number of approximately 4.3. This is well below the recognised threshold of 3000 at a flow rate in excess of the maximum applied within this thesis. It can be expected that laminar flow is present within the separation of an Owlstone FAIMS sensor through all investigations.

2.7 Position of ions within planar FAIMS

While the expressions describing drift velocity and mobility are important in understanding the underlying theory of FAIMS the treatment of the position of ions within the separation region can be more directly linked to operational parameters. Specifically, the expressions derived better describe the affect of the particular form of the applied asymmetric waveform beyond simply its magnitude.

2.7.1 Translational position of ion

The translational position of an ion after it enters the separation region of a FAIMS device is dependent upon the flow of the neutral carrier gas. The position of the ion between the electrodes is dependent upon the asymmetric waveform applied across the electrodes. The following discussion is based upon the account provided from Miller *et al*. [14].

The asymmetric waveform being considered in the following discussion is an idealised, simple high and low field asymmetric waveform. The theory can be applied to more complex waveforms but for this discussion the form of the waveform is that as depicted within Figure 2.5.

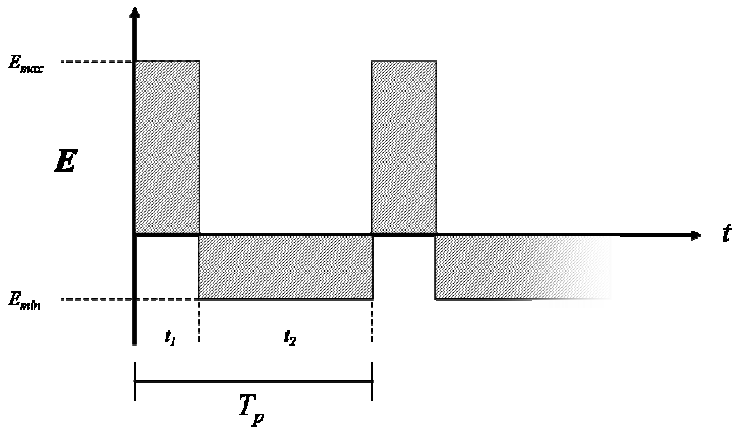

Figure 2.5 An idealised asymmetric waveform which complies with the conditions required for use within a FAIMS system. The waveform has a period of T_p and is made from two regions, one of high field strength and the other of low field strength in the opposite polarity.

It is known from the requirements of the asymmetric waveform that the product of the electric field strength and the time that the field is imposed must equal the same product in the opposite polarity.

$$|E_{\max}|t_1 = |E_{\min}|t_2 = \beta \qquad 1.5$$

Where β is a constant. A more rigorous treatment of what constitutes an appropriate waveform is discussed in Appendix F.

The longitudinal motion of the ion is in the *x*-axis and the transverse motion is in the *y*-axis, as defined in Figure 2.1. The velocity of the ion between the two electrodes of the separation region is dependent upon Equation 1.1, therefore,

$$v_y = K(E)E(t) \tag{2.36}$$

The velocity of the ion within the high field region ($E_{\max}$) of the applied asymmetric waveform is described by,

$$v_{E_{\max}} = K_{E_{\max}} \left| E_{\max} \right| \tag{2.37}$$

Likewise the velocity of the ion within the low field region ($E_{\min}$) of the applied asymmetric waveform is described by,

$$v_{E_{\min}} = K_{E_{\min}} \left| E_{\min} \right| \tag{2.38}$$

Also, the displacement between the electrodes (Δy) is dependent upon the transverse velocity (v_y) over a time Δt.

$$\Delta y = v_y \Delta t \tag{2.39}$$

By combining Equations 2.36, 2.37, 2.38 and 2.39 it is possible to obtain an expression for the motion of an ion between the electrodes of the separation region over the period of a single asymmetric waveform.

$$\Delta y = K_{E_{\max}} \left| E_{\max} \right| t_1 - K_{E_{\min}} \left| E_{\min} \right| t_2 \tag{2.40}$$

$$= K_{E_{\max}} \beta - K_{E_{\max}} \beta \tag{2.41}$$

$$= \beta \left(K_{E_{\max}} - K_{E_{\min}} \right) \tag{2.42}$$

$$= \beta \Delta K \tag{2.43}$$

Together, Equations 1.5 and 2.43 demonstrate why separation increases with an increase in applied electric field strength as β is directly proportional to E_{max}.

To understand the total transverse ion displacement across the separation region the period of the asymmetric waveform (T_p) is defined. T_p is simply the time of the high and low field regions summed together.

$$T_p = t_1 + t_2 \qquad 2.44$$

The total transverse displacement (Y) of an ion within the separation region can therefore be expressed to a first approximation as,

$$Y = v_y t_{res} = \frac{\Delta y}{T_p} t_{res} = \frac{\beta \Delta K}{T_p} t_{res} \qquad 2.45$$

The duty cycle (D_T) of the asymmetric waveform is defined as a fraction of when the waveform is in the high field region with respect to the total waveform period.

$$D_T = \frac{t_1}{T_p} \qquad 2.46$$

Substituting Equations 2.33, 2.40 and 2.46 into Equation 2.45 gives,

$$Y = \frac{\Delta K E_{\max} V D_T}{Q} \qquad 2.47$$

Equation 2.47 predicts that by increasing the maximum electric field strength within the separation region the transverse ion displacement will increase. This means that any ion species with a ΔK greater than zero will neutralise against an electrode quicker if it possesses a high mobility difference.

Miller *et al*. stated that the CV position is dependent on the flow rate as expressed through Equation 2.47 [14]. This assertion is disputed here since the total displacement of an ion within the separation region is different from the compensation voltage of a detected ion species. For detection an ion species must have made it through the separation region which requires a total translational displacement (Y) smaller than the gap height. This is made possible for ions of various mobilities through the application of a compensating field. Since the compensating field is continuously applied across the separation region, under the correct conditions for detection the transverse displacement of the ion will effectively be zero after each waveform and so is independent of the residence time and hence the flow rate. Experiments reported in Chapter 5 went on to investigate this in more detail.

2.7.2 Effective gap height

The drift velocity, which K within Equation 2.47 is dependent upon, still represents only the average drift velocity of the swarm. All ions within the separation region are susceptible to random interactions with the neutral carrier gas which can lead to premature neutralisation on an electrode surface.

An important outcome of the equations describing ion displacement during an applied waveform is the appreciation of a new loss mechanism for the ions of interest. For detection an ion requires a net displacement through the separation region of a FAIMS system less than the gap height. However, the ions with $\Delta K > 0$ will move towards or away from an electrode during a period of the waveform even without interaction with the neutral carrier flow (Equation 2.36). This means that ions of interest must actually have a net displacement less than an effective gap height [22]. This effective gap height is equal to

the gap height minus the maximum distance travelled by the ion of interest during a period of the asymmetric waveform. An example of the presence of an effective gap height is depicted in Figure 2.6.

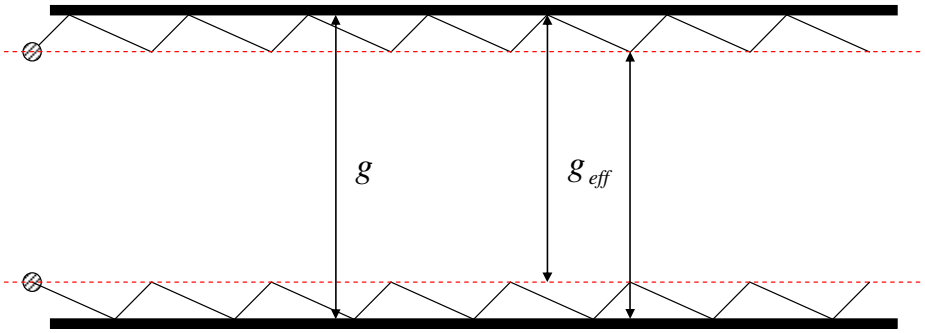

Figure 2.6 Cut away through the length of a separation region of a simple planar FAIMS device. Included are the theoretical paths of two ions of interest with the correct mobility characteristics as they travel through the device under the influence of an asymmetric waveform. The dashed red lines represent thresholds that the ions can not cross if they are to traverse the entire separation region.

The effective gap height of a separation region is therefore,

$$g_{eff} = g - y_{\max} \qquad 2.48$$

Where $y_{\max}$ is the maximum transverse ion displacement during either region of the asymmetric waveform.

2.7.3 Effect of changing the frequency of waveform

From Equation 2.40 the displacement of an ion is dependent upon the time spent in each portion of the waveform. For ions that increase in mobility in the high field region displacement per cycle of the waveform will increase the longer the high field is imposed. Section 2.7.2 described how this can lead to increased losses to the side walls of the separation region. Increasing the frequency of the waveform reduces the displacement of ions within a single waveform but still permits the same filtering of ions within the separation region.

The frequency (f) of the applied asymmetric waveform is related to the period of the same waveform by the expression,

$$T_p = \frac{1}{f} \qquad 2.49$$

Also the transverse ion displacement for the high field region is,

$$y_{E_{\max}} = K_{E_{\max}} |E_{\max}| t_1 \qquad 2.50$$

The maximum electric field strength can be expressed as,

$$E_{\max} = \frac{V_{\max}}{g} \qquad 2.51$$

Where $V_{\max}$ is the voltage of the idealised asymmetric waveform in the high field region.

Combining Equations 2.46, 2.49, 2.50 and 2.51 and then substituting into Equation 2.48 provides,

$$g_{eff} = g - \frac{V_{\max} D_T K_{E_{\max}}}{fg} \qquad 2.52$$

This is a simplification of the real losses incurred through this mechanism since it is based upon an idealised waveform but it is something that affects FAIMS systems. This is particularly true for designs with a small gap height since any loss translates to a greater percentage loss than for larger sensors. It is an obvious conclusion to state that for maximum transmission of ions of interest through the separation region g_{eff} should approximately equal g.

From this treatment it appears that only benefits can result from increasing the frequency. However, a very rapidly changing waveform (between low and high fields) is a violent

environment for a molecular-ion. FAIMS relies heavily on chemistry within the separation region which can be affected by the limits imposed on interaction times through a change in frequency. An example of this would be the phenomena of clustering (Section 2.3.5).

2.8 Modifying the geometry of electrodes

The separation of ions within a FAIMS instrument is dependent upon several interconnected quantities. Some of these quantities, such as electric field, are varied as part of the normal operation and can easily be tailored within certain limits. One quantity that affects all other considerations is that of electrode geometry and it cannot be changed following fabrication of a FAIMS system.

2.8.1 Modifying the width and length of the separation region

If the gap (or analytical) height is kept constant while the length and width are changed the position of resultant peaks with respect to CV remains unchanged. This is due to the ion's mobility coefficient being dependent upon the electric field experienced. In the case of a planar FAIMS device the electric field is applied orthogonally to the length and width of the separation region and therefore is independent of the changing geometry.

Maintaining the gap height while length and width are changed will modify the residence times of ions in accordance with Equation 2.33. This can affect the sensitivity and resolution but not the CV position of ions.

Another consideration is that changing the length of the separation region changes the angle of trajectory an ion has to possess for detection. A greater length would reduce the acceptance angle and hence reduce the FWHM. From geometric considerations the angle

of acceptance is not linear with length and the rate of change decreases with increased length. More accurately the angle of acceptance is dependent upon the ratio of the gap height with the length of the separation region.

$$\tan \gamma = \frac{g}{l} \qquad 2.53$$

Where γ is the acceptance angle.

2.8.2 Modifying the gap height of the separation region

Narrowing the gap height of the separation region decreases the volume. This leads to both an increase and decrease in the losses attributable to diffusion since both the residence time and effective gap height is reduced. This loss can be countered through an increase in frequency of the waveform (Section 2.7.3). The net trade-off will depend on the particular geometry.

There is another trade-off with respect to the separation of ions within the modified sensor. Narrowing the gap height would lead to an increased maximum electric field. This would alter the CV position at which ions are observed. Additionally, more ions of incorrect mobility would be lost because of the smaller effective gap height. However, reducing the gap height also decreases the residence time of ions which affects their net separation. Furthermore, the angle of acceptance of ions through the separation region is dependent upon the gap height as expressed through Equation 2.53 (Section 2.8.1).

2.9 Diffusional loss

Diffusion is the major loss mechanism for ions that have the correct mobility coefficient to traverse the FAIMS separation region. The random interactions which ions experience with the neutral carrier flow can lead to the ions of interest reaching an electrode surface and neutralising. This diffusion is dependent on a number of factors including, indirectly and directly, the geometry of the separation region. With a value of zero being complete ion transmission and a value of unity meaning total signal loss. The dimensionless diffusion loss is calculated through [22, 23],

$$Diffusion\ loss = 1 - \exp\left(\frac{-\pi^2 k_b T}{e}\frac{K t_{res}}{g_{eff}^2}\right) \qquad 2.54$$

Equation 2.54 can be simplified by considering the Einstein relation,

$$K = \frac{eD}{k_b T} \qquad 2.55$$

Where D is the diffusion coefficient.

Now the diffusion loss can be expressed as,

$$Diffusion\ loss = 1 - \exp\left(-\pi^2 D\left(\frac{t_{res}}{g_{eff}^2}\right)\right) \qquad 2.56$$

Equation 2.54 is of the general form,

$$1 - \exp(-A) \approx A \qquad 2.57$$

Where A is any expression and Equation 2.57 is only true for small values of A.

Therefore, for a small diffusion loss Equation 2.54 can again be simplified to,

$$Diffusion\ loss = \left(\pi^2 D\left(\frac{t_{res}}{g_{eff}^2}\right)\right) \qquad 2.58$$

Figure 2.7 is constructed from Equation 2.54 assuming an ion mobility of 0.8 $cm^2/V{\cdot}s$.

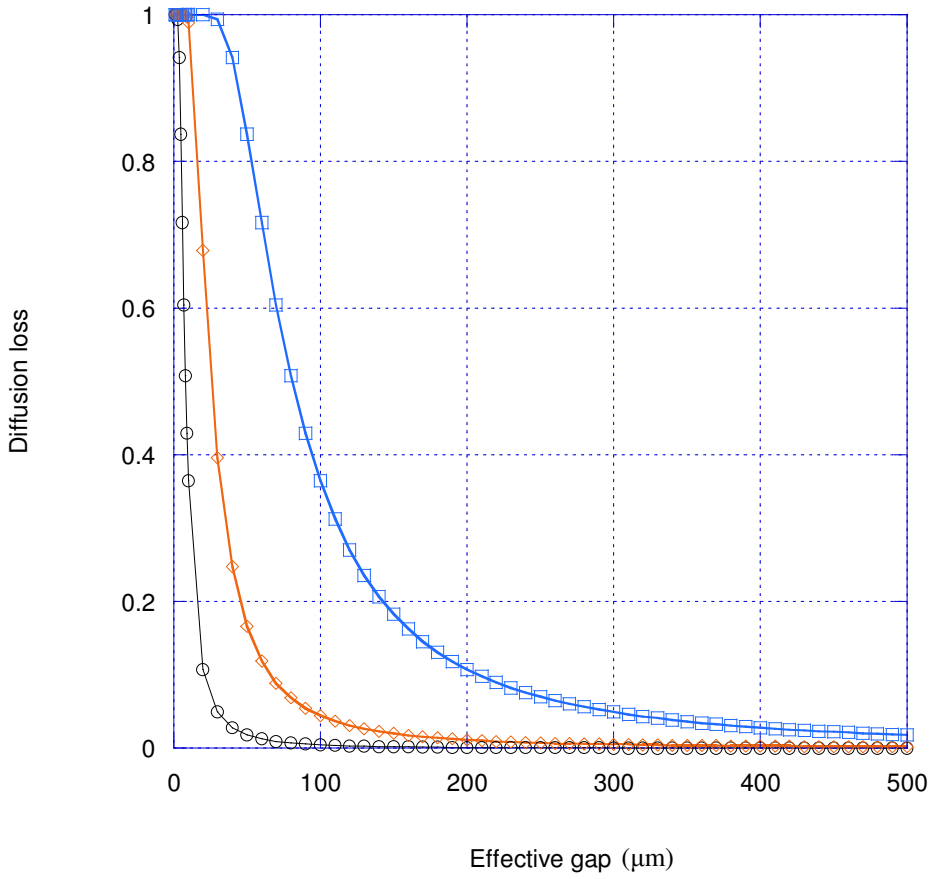

Figure 2.7 Diffusion loss at residence times of 2 μs (black circles), 20 μs (orange diamonds) and 200 μs (blue squares) as dependent on the effective gap.

Diffusion loss is of greater importance at low effective gap heights but the losses are reduced with a reduction in the residence time of ions within the separation region. It becomes clear that the quantities of residence time and the effective gap height are important when considering diffusion loss. These two quantities are controlled through the geometry of the separation region and the flow rate of the neutral carrier gas. The diffusion loss is proportional to the residence time and effective gap height through,

$$Diffusion\ loss \propto \frac{t_{res}}{g_{eff}^2} \qquad 2.59$$

As the residence time is decreased, sensitivity will be closer to optimum; if the effective gap height is reduced, the losses due to diffusion will markedly increase as Equation 2.59

is sensitive through the g_{eff}^2 term. The effect of narrowing the effective gap height is not wholly detrimental since the residence time is reduced through Equation 2.33.

2.9.1 Full width at half maximum (FWHM)

The resolution of ion responses is dependent upon the residence time of ions in the separation region. This means there is a dependence upon the dimensions of the separation region as described through Equation 2.33. A measure of how much an ion response is spread across a CV position is the full width at half maximum (FWHM) of that ion response. The greater the FWHM, the more likely multiple ion responses are to overlap with one another resulting in a loss of resolution. An expression for the FWHM of a peak from a FAIMS device in a low mobility regime is [22, 24],

$$FWHM = \frac{4}{K}\sqrt{\frac{D\ln 2}{t_{res}}} = 4\sqrt{\frac{k_b T \ln 2}{eKt_{res}}} \qquad 2.60$$

Where D is the diffusion coefficient and substitution with Equation 2.55.

Shvartsburg states at 'extreme' electric fields the FWHM will become dependent on both the magnitude and profile of the applied waveform [24]. There is however no criteria given as to what level a high strength field can be considered of extreme strength.

Figure 2.8 was constructed with Equation 2.60 using a temperature of 300 K and mobility coefficient of 0.8 $cm^2/V{\cdot}s$.

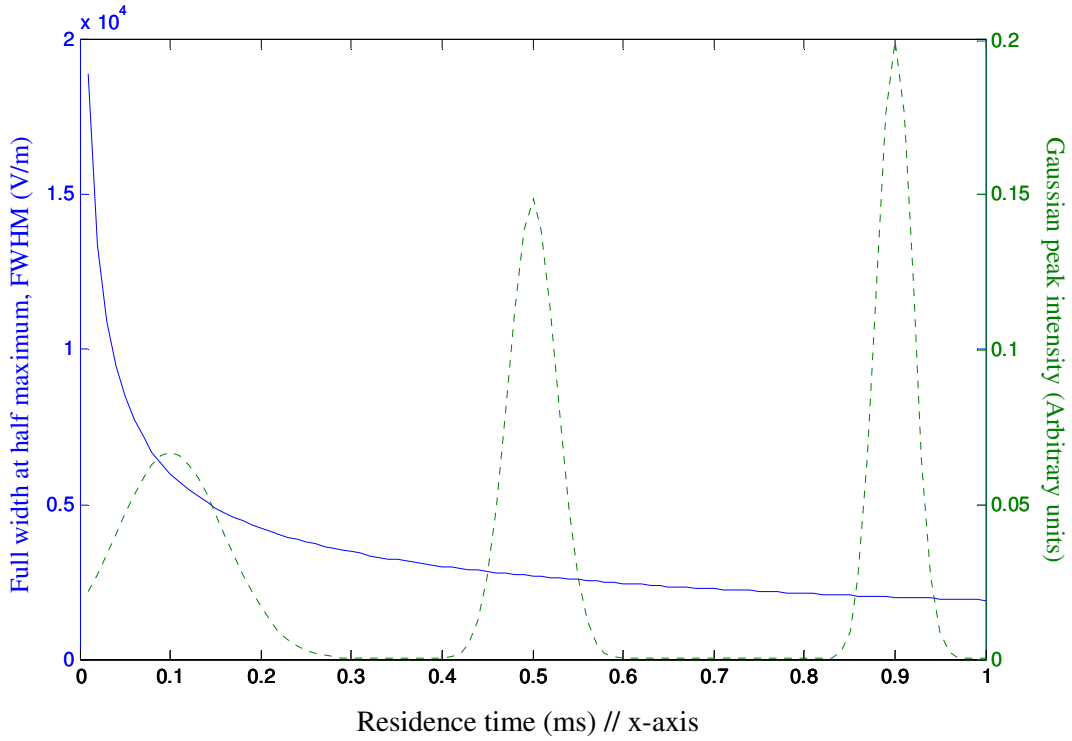

Figure 2.8 FWHM values for residence times between 0.01 - 1 ms (solid blue). Three Gaussian peaks (dashed green) of area unity have been plotted at residence times 0.1, 0.5 and 0.9 ms. The FWHM of those Gaussian peaks are calculated from Equation 2.60 using the residence time of their position on the x-axis.

As well as a plot of FWHM over a range of residence times three ion responses of area unity have been plotted. Each ion response is centred upon the residence time used to calculate their FWHM. At a lower FWHM it is less likely that ion responses of different mobility will overlap one another, thus improving the potential resolution of the analysis. Figure 2.8 also shows that as the residence time is increased the rate of benefit garnered through a reduction in the FWHM decreases.

Increasing the gap height while also decreasing the flow rate would improve sensitivity and resolution. However, through an increase in gap height an increase in the voltage across the separation region would be required to maintain an equivalent electric field. There is a limit to the extent the voltage can be increased across the separation region (beyond practical limitations) which is described by Paschen's law (Section 2.10.1).

2.10 Imposed limits of operation

Beyond the theory developed to describe ion mobility the operation of FAIMS is also affected by common phenomena. Within this section important limitations not directly addressed through ion mobility theory is discussed.

2.10.1 Breakdown voltage and Paschen's law

The partition of ions within the separation region of a FAIMS instrument is dependent upon the magnitude of the electric field that the ions experience. The electric field within the separation region is increased through the voltage applied between the electrodes. The voltage can not be amplified *ad infinitum* since there will be a case where an arc will travel from one electrode to the other. Such an arc occurs when the medium between the electrodes exceeds its 'breakdown voltage'. At the breakdown point the voltage is too great for the supporting atmosphere (for a FAIMS system this will be the carrier gas) and the insulating medium becomes electrically conductive. This is described by Paschen's law [25].

Paschen's law

$$V_B = \frac{a(Pg)}{\ell n(Pg) + b} \qquad 2.61$$

Where V_B is the breakdown voltage, and a and b are constants dependent upon the identity of the carrier gas. With regard to air at atmospheric pressure, Paschen's law does not describe the breakdown voltage well at gap heights below 10 μm [26, 27].

Figure 2.9 shows the breakdown voltage over a range of pressure × gap height (Pg) where the minimum of the resultant curve is the breakdown voltage, and therefore the maximum voltage that should be employed within the separation region.

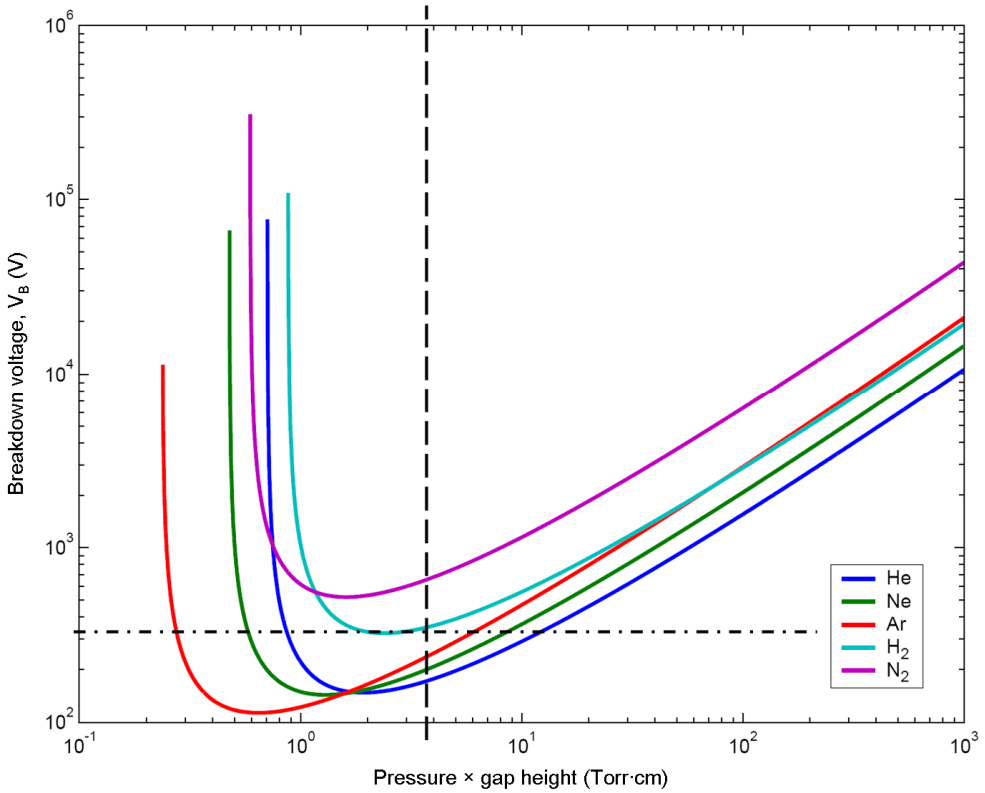

Figure 2.9 Breakdown voltage against a range of pressure × gap Height for various gasses. Dashed black line corresponds to *Pg* of Owlstone FAIMS device at one atmosphere. Dot-dash line corresponds to maximum voltage applied across separation region in Owlstone FAIMS sensor.

As long as the maximum applied across a separation region is below V_B, decreasing the gap height enables ever greater electric fields to be imposed without risking an arc across the electrodes. A small gap height therefore enables greater electric fields with comparable resources to devices with larger geometry. While there is a trade-off attributable to reducing the gap height with regards to ion losses by diffusion (Section 2.9) the breakdown voltage imposes an absolute maximum that the gap height can be increased.

2.10.2 Space charge effect

The major cause for ion swarm broadening within a FAIMS system is thermal diffusion. A second reason for broadening is Coulomb repulsion of ions of like charge. This is known as the space charge effect.

The magnitude of the space charge effect is proportional to the square of the charge density. When the charge density is too great the repulsion of like ions to the walls of the FAIMS sensor, within the residence time of the separation region, results in neutralisation. The space charge effect therefore not only affects the resolution but also imposes a limit on the maximum current permissible. This limit is known as the charge capacity [10].

In traditional IMS devices space charge effects are normally surpassed by the larger effect of thermal diffusion [28]. With the development of FAIMS, greater duty cycles, smaller analytical volumes and improvements in ionisation efficiencies space charge effects are increasingly becoming significant, Shvartsburg calls for further research [10].

Charge density can be reduced by streaming ions into multiple channels, since the repulsion is described by Coulomb's law,

Coulomb's law

$$F_C = \frac{1}{4\pi\varepsilon_0}\frac{q^2}{r^2} = k_c\frac{q^2}{r^2} \qquad 2.62$$

Where ε_0 is the permittivity of free space, r is the distance between ions, q is the charge on an ion and k_c is the proportionality constant for the expression.

The q^2 dependence ensures that as the ions are divided into separate channels the repulsion they experience is greatly reduced. Minimisation of the residence time is also beneficial since it provides less time for ion swarms to expand under the space charge effect. Dividing the separation region into multiple channels therefore greatly limits the occurrence of the space charge effect [10].

2.11 Conclusion

This chapter has explored many of the key considerations when assessing the operation of a FAIMS device. Through an understanding of how the eventual response from a FAIMS analysis is dependent upon a host of factors a more informed and confident assessment of data can be made.

Furthermore, an appreciation of how a change in geometry affects the properties of a FAIMS sensor was highlighted and occasionally explored. Many of the expressions resulted in a series of trade offs where the net effect being positive or negative depended upon a number of additional parameters. The work reported on in the remainder of this thesis predominantly deals with the Owlstone FAIMS sensor which utilises a smaller geometry than previous systems. This review of theory will therefore be invaluable in explaining some of the effects observed with its operation.

Also, a potential avenue that appears worthwhile of exploration is the restriction of the acceptance angle by increasing the separation region length while maintaining the gap height. This will reduce the FWHM (Section 2.8.1) but also increase losses attributable to diffusion. This could be independently countered through increasing the rate of the carrier flow to maintain the previous residence time (Section 2.6.1). The modifications do not change the energy that the ions experience from the original configuration so the CV positions should be equivalent to previous investigations and the system should be at similar sensitivity while exhibiting increased resolution.

2.12 References

1. Good, A., Durden, D.A., and Kebarlf, P., *Ion-Molecule Reactions in Pure Nitrogen and Nitrogen Containing Traces of Water at Total Pressures 0.5 - 4 torr. kinetics of Clustering Reactions Forming H+(H2O)n.* The Journal of Chemical Physics, 1969. **52**(1): p. 212 - 221.
2. Eiceman, G.A. and Karpas, Z., *Ion Mobility Spectrometry*. Second ed. 2005: Taylor & Francis. 350.
3. Bell, S.E., Ewing, R.G., Eiceman, G.A., and Karpas, Z., *Atmospheric pressure chemical ionization of alkanes, alkenes, and cycloalkanes.* Journal of the American Society for Mass Spectrometry, 1994. **5**(3): p. 177-185.
4. Eiceman, G.A., *The reaction chemistry and mobility of gas phase ions in air at ambient pressure for chemical measurements and characteristaion of ion-molecule associations*. 2010: Analytical Research Forum 2010, Loughborough University.
5. Nazarov, E.G., Coy, S.L., Krylov, E.V., Miller, R.A., and Eiceman, G.A., *Pressure effects in differential mobility spectrometry.* Analytical Chemistry, 2006. **78**(22): p. 7697-7706.
6. Mason, E.A. and McDaniel, E.W., *Transport Properties of Ions in Gases*. 1988: Wiley, New York.
7. Eiceman, G.A., Bergloff, J.F., Rodriguez, J.E., Munro, W., and Karpas, Z., *Atmospheric pressure chemical ionization of fluorinated phenols in atmospheric pressure chemical ionization mass spectrometry, tandem mass spectrometry, and ion mobility spectrometry.* Journal of the American Society for Mass Spectrometry, 1999. **10**(11): p. 1157-1165.
8. Marcis, Y., *Ion Solvation*. 1985: Wiley - Interscience.
9. Krylova, N., Krylov, E., Eiceman, G.A., and Stone, J.A., *Effect of moisture on the field dependence of mobility for gas-phase ions of organophosphorus compounds at atmospheric pressure with field asymmetric ion mobility spectrometry.* Journal of Physical Chemistry A, 2003. **107**(19): p. 3648-3654.
10. Shvartsburg, A.A., *Differential Ion Mobility Spectrometry*. 2009, Boca Raton: CRC Press, Taylor and Francis Group.
11. Viitanen, A.K., Mattila, T., Makela, J.M., Marjamaki, M., Anttalainen, O., and Keskinen, J., *Experimental study of the effect of temperature on ion cluster formation using ion mobility spectrometry.* Atmospheric Research, 2008. **90**(2 - 4): p. 115 - 124.
12. Rorrer III, L.C. and Yost, R.A., *Solvent vapor effects on planar high-field asymmetric waveform ion mobility spectrometry.* International Journal of Mass Spectrometry, 2010.
13. Eiceman, G.A., Krylov, E.V., Krylova, N.S., Nazarov, E.G., and Miller, R.A., *Separation of Ions from Explosives in Differential Mobility Spectrometry by Vapor-Modified Drift Gas.* Analytical Chemistry, 2004. **76**(17): p. 4937-4944.
14. Miller, R.A., Nazarov, E.G., Eiceman, G.A., and King, A.T., *A MEMS radio-frequency ion mobility spectrometer for chemical vapor detection.* Sensors and Actuators a-Physical, 2001. **91**(3): p. 301-312.
15. McDaniel, E.W. and Mason, E.A., *The Mobility and Diffusion of Ions in Gases*. 1973: Wiley. 372.
16. Hirschfelder, J.O., Curtiss, C.F., and Bird, R.B., *Molecular Theory of Gases and Liquids*. 1954: John Wiley & Sons, Inc. 1249.
17. Wannier, G.H., *Motion of Gaseous Ions in Strong Electric Fields.* Bell System Technical Journal, 1953. **32**: p. 170 - 254.

18. Miller, R.A., Eiceman, G.A., Nazarov, E.G., and King, A.T., *A novel micromachined high-field asymmetric waveform-ion mobility spectrometer.* Sensors and Actuators B: Chemical, 2000. **67**(3): p. 300-306.
19. Basanta, M., Singh, D., Fowler, S., Wilson, I., Dennis, R., and Thomas, C.L.P., *Increasing analytical space in gas chromatography-differential mobility spectrometry with dispersion field amplitude programming.* Journal of Chromatography A, 2007. **1173**(1-2): p. 129-138.
20. Eiceman, G.A., Tadjikov, B., Krylov, E., Nazarov, E.G., Miller, R.A., Westbrook, J., and Funk, P., *Miniature radio-frequency mobility analyzer as a gas chromatographic detector for oxygen-containing voltaile organic compounds, pheromones and other insect attractants.* Journal of Chromatography A, 2001. **917**: p. 205 - 217.
21. Elistratov, A.A., Shibkov, S.V., and Nikolaev, E.N., *Analysis of non-linear ion drift in spectrometers of ion mobility increment with cylindrical drift chamber.* European Journal of Mass Spectrometry, 2006. **12**(3): p. 153 - 160.
22. Krylov, E.V., Nazarov, E.G., and Miller, R.A., *Differential mobility spectrometer: Model of operation.* International Journal of Mass Spectrometry, 2007. **266**(1-3): p. 76-85.
23. Shi, Q., Anderson, A., Morris, J., Coy, S., Krylov, E., and Nazarov, E., *Adjusting DMS design for particular applications: optimizing RF waveform, construction and sensor dimensions*. 2009: ISIMS 2009, Thun, Switzerland.
24. Shvartsburg, A.A., Smith, R.D., Wilks, A., Koehl, A., Ruiz-Alonso, D., and Boyle, B., *Ultrafast Differential Ion Mobility Spectrometry at Extreme Electric Fields in Multichannel Microchips.* Analytical Chemistry, 2009. **81**(15): p. 6489–6495.
25. Paschen, F., *Ueber die zum Funkenübergang in Luft, Wasserstoff und Kohlensäure bei verschiedenen Drucken erforderliche Potentialdifferenz.* Annalen der Physik, 1889. **273**(5): p. 69-96.
26. Hourdakis, E., Simmonds, D.J., and Zimmerman, N.M., *Submicron gap capacitor for measurement of breakdown voltage in air.* Review of Scientific Instruments, 2006. **77**.
27. Hourdakis, E., Bryant, G.W., and Zimmerman, N.M., *Electrical breakdown in the microscale: Testing the standard theory.* Journal of Applied Physics, 2006. **100**.
28. Spangler, G.E., *Space Charge Effects in Ion Mobility Spectrometry.* Analytical Chemistry, 1992. **64**: p. 1312.